J Mater Sci (2007) 42:5426–5430
DOI 10.1007/s10853-006-0772-6

Hollow biomorphic Al_2O_3 fibers produced from sisal

Tarcisio E. Andrade Jr · Carlos Renato Rambo · Heino Sieber · Antonio E. Martinelli · Dulce Maria A. Melo

Received: 9 March 2006 / Accepted: 7 August 2006 / Published online: 28 March 2007

Abstract Al_2O_3 fibers with a hollow morphology were produced by Al-vapor infiltration-reaction and subsequent oxidation from pyrolysed fibers of natural sisal. Following pyrolysis, the bio-fiber template was reacted with gaseous Al at 1,400 °C–1,600 °C in vacuum to form Al_4C_3. After an oxidation/sintering process at 1,550 °C, the biomorphic Al_4C_3 fibers were fully converted into Al_2O_3, maintaining the microstructural features of the native sisal. Phase and microstructural characterization during processing were evaluated by high temperature X-ray diffractometry and scanning electron microscopy, respectively. Thermo-analyses were performed in the Al_4C_3 samples in order to estimate the reactions and the weight change during the oxidation step.

Introduction

Sisal is a widely used natural resource and one of the major natural fibers produced worldwide. The low-cost and biodegradable lignocellulosic fibers are extracted from sisal and commonly used in the manufacture of both handcrafted and industrial goods including ropes, mats and carpets. Alternatively, added-value products can be industrialized using sisal as a low-cost engineering material. The sisal plant is very easily cultivated, has short renewal times and grows wild in the hedges of fields and railway tracks [1]. Nearly 4.5 million tons of sisal fibers are produced every year throughout the world. Tanzania and Brazil are the two main sisal-producing countries, but tropical countries of Africa and the West Indies are also world producers [2]. The fiber is hard and extracted from the leaves of the sisal plant (*Agave sisalana*). A sisal plant produces about 200–250 leaves and each leaf contains 1,000–1,200 fiber bundles (sclerenchyma fibers), composed of 4% fiber, 0.75% cuticle, 8% dry matter and 87.25% water. Usually, a leaf weighting 600 g yields 3 wt.% of fiber with each leaf containing about 1,000 fibers [1].

Sisal is also a very interesting low cost, renewable engineering material. The high specific strength and modulus allied to the low density of sisal fibers have attracted the interest for technological applications [3–5]. Several recent studies have reported on the use of sisal fibers in engineering applications such as reinforcement for composites including cement [6] and polymers like polypropylene [7], rubber [8] and starch [9]. The hierarchical anatomy of sisal fibers is also an attractive template for the design of cellular ceramic fibers. Naturally grown plants (wood, fibers or grass) exhibit a unique porous microstructure with a wide range of pore anatomies that are interesting for structural applications [10] and for the conversion into advanced engineering materials [11]. The conversion (biotemplating) of native tissues into biomorphic ceramics with hierarchical, microcellular morphology is based on two processing approaches: substitution and transformation. Substitution is achieved by coating the

T. E. Andrade Jr · A. E. Martinelli (✉) · Dulce Maria A. Melo
Department of Chemistry, Federal University of Rio Grande do Norte, 59072-970 Natal, RN, Brazil
e-mail: aemart@uol.com.br

C. R. Rambo
Chemical Engineering Department, Federal University of Santa Catarina, P.O. Box 476, 88040-900 Florianópolis, SC, Brazil

H. Sieber
Department of Materials Science, Glass and Ceramics University of Erlangen-Nuremberg, Martensstrasse, 5, 91058 Erlangen, Germany

inner surfaces of the plant tissue with oxidic precursors [12–14]. Burning the template in air releases carbon as CO/CO_2 and promotes its consolidation into an oxide ceramic. Transformation involves the direct conversion of the carbonized template by reaction into carbide phases [15–20]. The synthesis of porous Al_2O_3-ceramics with unidirectional oriented pores from conventional technologies was also reported in the literature, e.g., by the coating of cotton fibers with an alumina slurry [21] or by the formation of oriented hydrogen bubbles in an alumina-sol-aluminum slurry [22].

However, with the increase of the microstructure complexity, e.g., multi-modal pore distribution in the micro- and nanometer range well oriented pore structures or complex cell geometries, technology and cost barriers have yet to be better unraveled. The manufacturing of complex microstructures is limited by consolidation and grain growth of alumina during the sintering process. Therefore, a compromise between the precision of the microstructure and the desired properties has to be established. This work reports on the conversion of natural sisal fibers into Al_2O_3 fibers via Al-gas infiltration/oxidation. This approach is described in a previous work [23]. Metal–vapor infiltration offers the facility to infiltrate porous templates with pore sizes down to the nanometer range, unreachable by the infiltration of melts or low viscosity suspensions. Gaseous infiltration could be more efficient to reproduce the biostructure in the micrometer scale down to few hundred nanometers.

Experimental

Sisal fibers (*Agave sisalana perrine*) were used as biological templates for manufacturing of biomorphic Al_2O_3 oxide ceramic. *In natura* sisal fibers were washed in double distilled water, dried at 100 °C for 24 h, cut and separated in bundles of 10 cm in length with approximately 1,000 fibers. The samples were pyrolysed at 800 °C for 1 h in N_2-atmosphere to decompose the biopolymers (cellulose, hemicellulose and lignin) into carbon. During pyrolysis a slow heating rate (1.5 K/min) was employed to avoid damages of the sisal cell walls. Subsequently, the carbonized templates were disposed above an Al-powder bed (*Alfa Aesar*, -325mesh, purity 99.5%) in an Al_2O_3-crucible without contact to the powder. The system was placed in a conventional tube furnace and submitted to an Al-vapor phase infiltration process at temperatures up to 1,600 °C for 1 h under vacuum (1–0.1 Pa) for reaction of the carbonized specimens into Al_4C_3. Immediately after cooling, the fibers were oxidized at temperatures up to 1,600 °C for 2 h at a heating rate of 10 °C/min. Details of the Al infiltration process are described elsewhere [23, 24].

Thermogravimetric analysis (TGA/DTA, 951 Thermogravimetric Analyzer, Du Pont Instruments, Wilmington/USA) was performed to evaluate the crystallization reaction and the total weight loss during thermal processing. DTA and TGA measurements were performed in the Al_4C_3 samples in order to estimate the reactions and the weight change during oxidation. The presence of crystalline phases was identified by X-ray diffraction using CuKα radiation (XRD, D 500, Siemens, Karlsruhe/Germany). The microstructure of the products were characterized by scanning electron microscopy (SEM, Phillips XL30).

Results and discussion

Figure 1 shows cross-section SEM images of a typical *in natura* (Fig. 1a) and a pyrolysed ribbon sisal fiber (Fig. 1b). The ribbon fibers are associated to the conductive tissue, composed by phloem and xylem vessels. The anatomy of the sisal fibers is characterized by a multicellular composition with small individual cells, the ultimate cells, longitudinally disposed and bonded together [1, 5]. These ultimate cells are the reinforcements for hemicellulose and lignin matrices. After pyrolysis, the anatomy of the fibers is maintained and the cellular morphology can be identified in detail. The conductive vessels are clearer seen in Fig. 1b. These are characterized by polygonal morphology and rounded lumen, as indicated by the arrow in Fig. 1b. The cells are more open due to the loss of organic

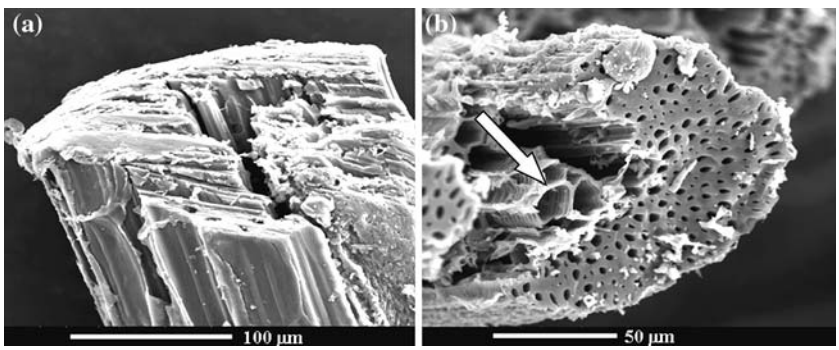

Fig. 1 SEM micrographs of: (**a**) raw sisal fiber and (**b**) pyrolysed sisal (ribbon) fiber

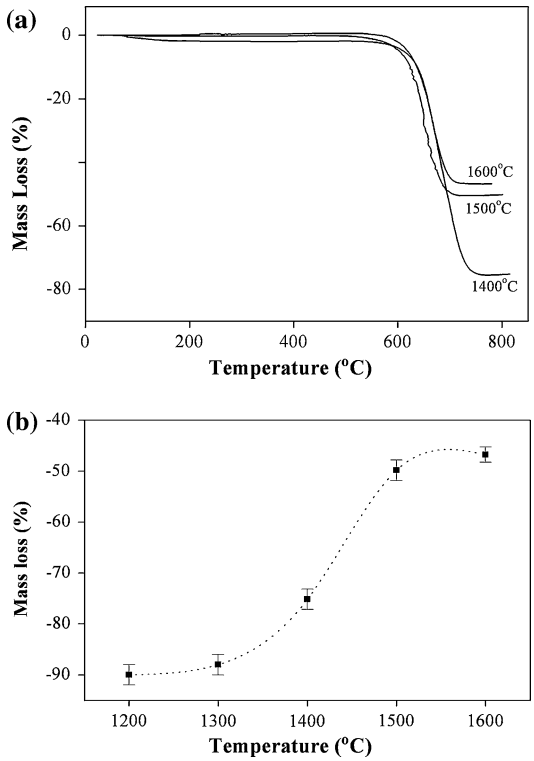

Fig. 2 Thermal behavior by annealing in air of biomorphic Al_4C_3 after Al-infiltration at different temperatures. (**a**) TGA curves up to 800 °C and (**b**) Measured mass loss after oxidation at 800 °C

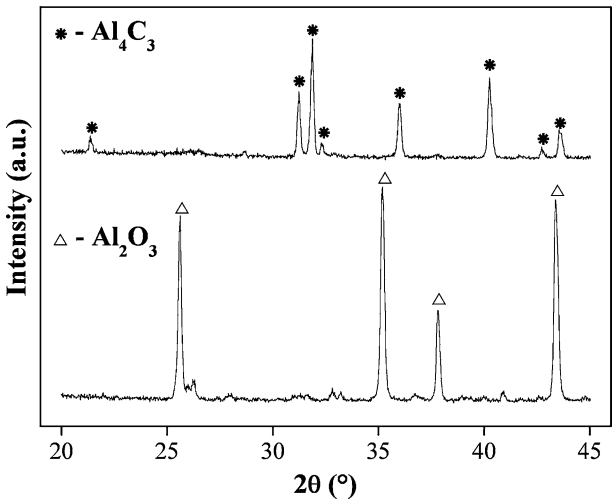

Fig. 3 XRD analysis of biomorphic reaction products after Al-vapor infiltration at 1,600 °C/1 h and after oxidation/sintering in air at 1,600 °C/3 h (*—Al_4C_3, Δ—Al_2O_3)

mass during pyrolysis, which facilitates the infiltration of Al-gas. Figure 2 shows the thermal behavior of the biomorphic Al_4C_3 product, after Al-gas infiltration at different temperatures. Figure 2a shows the TGA curves of the biomorphic Al_4C_3 by annealing in air up to 800 °C, after Al gas infiltration at 1,400 °C, 1,500 °C and 1,600 °C. No significant differences can be observed in the profile of the curves. Oxidation starts at 590–600 °C with the same rate and ended at around 700 °C. Above 750 °C, no mass loss was observed for all samples. Figure 2b shows the final mass loss of the biomorphic Al_4C_3 specimen after Al-infiltration at temperatures from 1,200–1,600 °C. The mass loss after oxidation varied from 90% to 47% after infiltration at 1,200 °C and 1,600 °C, respectively. At 1,200 °C and 1,300 °C, only a surface reaction and no infiltration occurred, as evidenced by the high amount of carbon released by oxidation. The mass loss after oxidation at 800 °C significantly decreased (~30%) as the infiltration temperature increased from 1,400 °C to 1,600 °C, which indicates a higher Al_4C_3 yield after Al infiltration, resulting in less remaining carbon. Therefore, the temperature chosen for the infiltration process was 1,600 °C. Figure 3 shows the XRD-spectra of rattan-derived Al_4C_3- and Al_2O_3-ceramic samples after Al-vapor infiltration/reaction and oxidation/sintering, respectively. After Al-vapor infiltration/reaction, the biocarbon template was converted into rhombohedral Al_4C_3 (JCPDS 79–1736). Here, the sisal derived carbon template (C_B) reacted with gaseous Al to form Al_4C_3. Thus the C_B structure was fully converted into the carbide phase by the reaction:

$$4Al(g) + 3C(s) \rightarrow Al_4C_3 \quad \Delta G_{1,600\,^\circ C} = -113\ \text{Kcal} \tag{1}$$

Usually Al_4C_3 is an undesirable degradation product, which is well known to decrease the mechanical properties of composite materials and is unstable under moisture containing atmospheres [25], Eq. 2 shows the reaction products when Al_4C_3 reacts with air moisture:

$$Al_4C_3 + 18H_2O \rightarrow 4Al(OH)_3 + 3CO_2 + 12H_2 \quad \Delta G_{25\,^\circ C} = -304.4\ \text{Kcal} \tag{2}$$

However in this work, Al_4C_3 was simply an intermediary phase necessary for the conversion of biocarbon C_B-templates into Al_2O_3. Oxidation of the biomorphic Al_4C_3-specimens in air yielded the conversion into α-Al_2O_3:

$$2Al_4C_3 + 9O_2 \rightarrow 4Al_2O_3 + 6CO \quad \Delta G_{1,000\,^\circ C} = -1470.4\ \text{Kcal} \tag{3}$$

Due to Ca impurities, originally present in the sisal plant (CaO represents more than 50 wt.% of the ash composition) [13], a small amount of Ca-containing oxide was formed after oxidation. The small peaks in the Al_2O_3 spectrum were identified as $CaAl_{12}O_{19}$. The microstructure of biomorphic Al_2O_3 fibers can be seen in Fig. 4. Basically, two different types of fibers are present:

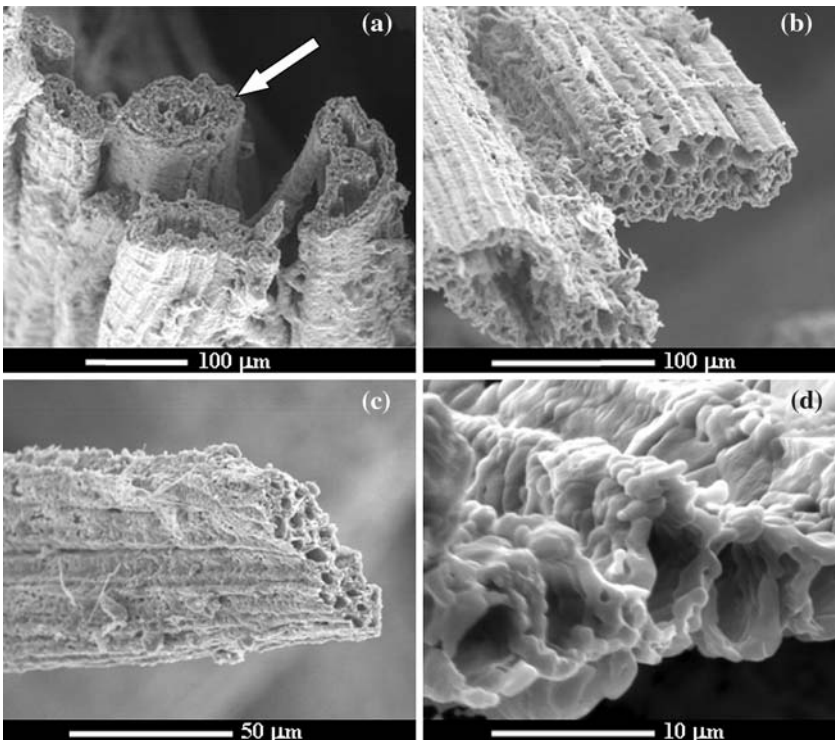

Fig. 4 SEM micrographs of biomorphic Al_2O_3 fibers (axial cuts)

mechanical and ribbon fibers. The mechanical fibers are ellipsoidal, with mean equivalent diameter of 100 μm (in the order of few mm in length) and are the predominant type (arrow in Fig. 4a). The ribbon fibers are the longest type and exhibit peanut-like shape (Fig. 4b and c) with approximately the same equivalent diameter. The conductive vessels (phloem and xylem) were well reproduced in the biomorphic Al_2O_3 fibers as can be seen in Fig. 4b. Although some loss of the parenchyma cells occurred in some of the fibers during oxidation, due to incomplete infiltration, the anatomy of the fibers was well maintained after the process. A single ribbon fiber is shown in Fig. 4c, evidencing the conductive (xylem) vessels. The conductive vessels are shown in detail in Fig. 4d. Cells with diameter of 5 μm, composed by Al_2O_3 grains with sizes ranging from 1–4 μm can be seen. The grains are sintered together, providing a dense ceramic cell wall, which gives mechanical stability to handle.

Figure 5 shows transversal cuts of the biomorphic Al_2O_3 fibers. A fiber with cross size of 100 μm can be seen. The fiber is composed of long parenchyma cells and conductive vessels. Microstructure and details of the transversal surface anatomy of a ribbon fiber is shown in Fig. 5b. Ultimate cells, with sizes of approximately 30 μm in length, uniformly disposed along the fiber are displayed. The cell-wall thickness is equivalent to the size of 1–3 layers of Al_2O_3 grains (2–10 μm). The reproduction of the original sisal anatomy down to the micrometer scale allowed to obtain hollow, vascular ceramic fibers with cellular morphology, which could be potentially applicable to fluid

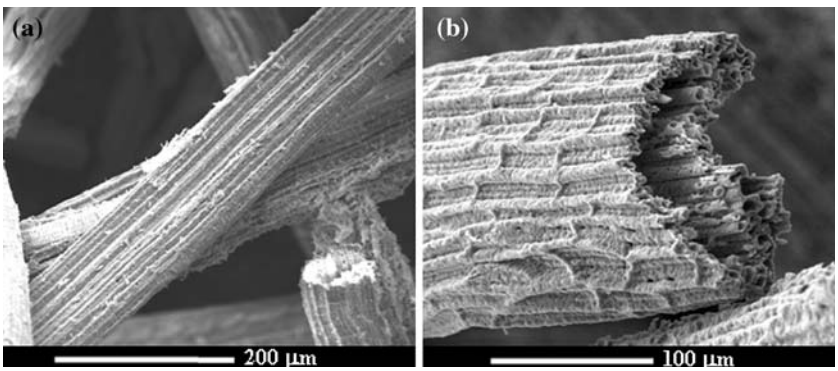

Fig. 5 SEM micrographs of the biomorphic Al_2O_3 fibers (transversal cuts)

filtration processes, where the fibers are dispersed (with or without preferential orientation) in a matrix, acting as reinforcement in a composite material.

The biodiversity of the natural plants from Brazil offers a large variety of different microstructures that can be converted into ceramics. The developed process can be applied to convert other biostructures (fibers and other plants), maintaining their natural morphological features. Cellular oxide ceramics with uniaxial pore structures and anisotropic properties could be of particular interest for applications in low-density heat insulation structure as well as catalyst carrier or substrates in high-temperature processes.

Summary

Hollow Al_2O_3 fibers were successfully produced by a 2-step processing from pyrolysed sisal fibers: (i) Al-vapor infiltration in vacuum at 1,600 °C, where the bio-fibers template reacted with gaseous Al to form Al_4C_3. (ii) Oxidation/sintering at 1,550 °C, to convert the biomorphic Al_4C_3 fibers fully into Al_2O_3. Although some loss of the parenchyma cells occurred in some of the fibers during oxidation, due to incomplete infiltration, the anatomical features of sisal fibers were well reproduced in the Al_2O_3 fibers down to the micrometer level and could be potentially useful in fluid filtration processes.

Acknowledgements The authors thank the Volkswagen Foundation for the financial support under contract I / 73 043 and CNPq Process no. 476817-03-4. Tarcisio E. Andrade Jr. also thanks CAPES/DAAD for a scholarship grant.

References

1. Murherjee PS, Satyanarayana KG (1984) J Mater Sci 19:3925
2. Chand N, Tiwary RK, Rohatgi PK (1988) J Mater Sci 23:381
3. Li Y, Mai Y-W, Ye L (2000) Compos Sci Technol 60:2037
4. Bisanda ETN, Ansell MP (1992) J Mater Sci 27:1690
5. Carvalho RF (2005) Ph.D. Thesis, USP, São Carlos, Brazil
6. Tolêdo Filho RD, Joseph K, Ghavami K, England GL (1999) Revista Brasileira de Engenharia Agrícola e Ambiental 3:245
7. Zhou XP, Li RKY, Xie XL, Tjong SC (2006) J Compos Mater 40:21
8. Martins MA, Joekes I (2003) J Appl Polym Sci 89:2507
9. Alvarez V, Vázquez A, Bernal C (2006) J Compos Mater 40:21
10. Gibson LJ (1992) Met Mater 8:333
11. Sieber H, Singh M (2005) In: Colombo P, Scheffler M (eds) Cellular ceramics—Structure, manufacturing, properties and applications. Wiley VCH Verlag GmbH, Weinheim/Germany p 122
12. Ota T, Imaeda M, Takase H, Kobayashi M, Kinoshita N, Hirashita T et al (2000) J Am Ceram Soc 83:1521
13. Cao J, Rambo CR, Sieber H (2004) Ceram Inter 30:1967
14. Rambo CR, Cao J, Sieber H (2004) Mat Chem Phys 87:345
15. Byrne CE, Nagle DE (1997) Mat Res Innovat 1:137
16. Greil P (2001) J Eur Ceram Soc 21:105
17. Greil P, Lifka T, Kaindl A (1998) J Eur Ceram Soc 18:1961
18. Vogli E, Mukerji J, Hoffmann C, Kladny R, Sieber H, Greil P (2001) J Am Cer Soc 84:1236
19. Vogli E, Sieber H, Greil P (2002) J Eur Ceram Soc 22:2663
20. Rambo CR, Cao J, Rusina O, Sieber H (2005) Carbon 43:1174
21. Zhang GJ, Yang JF, Ohji T (2001) J Am Ceram Soc 84:1395
22. Ding XJ, Zhang JZ, Wang RD, Feng CD (2002) J Eur Ceram Soc 22:411
23. Rambo CR, Sieber H (2005) Adv Mater 17:1088
24. Rambo CR, Mueller FA, Mueller L., Sieber H, Hofmann I, Greil P (2006) Mater Sci Eng C 26:92
25. Park JK, Lukas JP (1997) Scripta Mater 37:511